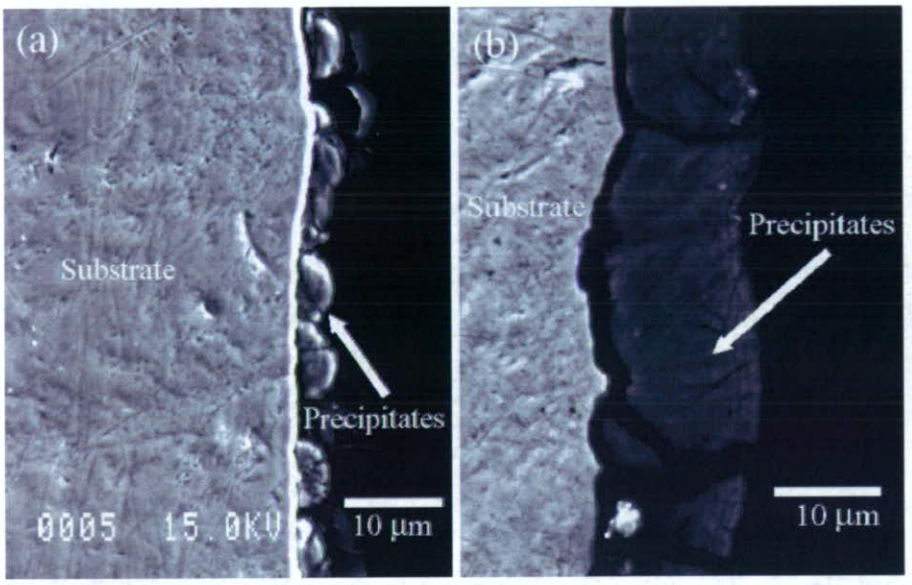

Figure 6. Typical SEM-images of cross sections of the specimens with (a) M2-stage and (b) M4-stage.

was observed on the surface of the cpTi side, and new bone [black asterisks in Fig. 9(a)] was formed away from the surface. Osteoblasts [arrowheads in Fig. 9(a)] were recognized on the surface of new bone tissue [Fig. 9(a)]. On the other hand, newly formed bone [black asterisks in Fig. 9(b)] was directly in contact with the surface of on the $CaTiO_3$ side, and many osteoblasts with a square cell shape [arrow heads in Fig. 9(b)] were observed on the osteoid [white arrows in Fig. 9(b)] formed on it [Fig. 9(b)]. On day 28, newly formed bone [black asterisk in Fig. 9(c)] on the cpTi side was remodeled to thinner, while it contacted with the surface directly [Fig. 9(c)]. In addition, on the $CaTiO_3$ side, bone remodeling on the surface progressed, and new bone [black asterisk in Fig. 9(d)] became thinner, as on the cpTi side [Fig. 9(d)].

Figure 10 shows osteogenesis around the specimen in bone marrow on day 7 by fluorescent microscopy. On the cpTi side, a slight amount of TC was deposited on the new bone away from the surface of the specimen [Fig. 10(a)]. On the other hand, in the $CaTiO_3$ film side, diffused TC deposition was observed on the new bone formed directly on the surface [Fig. 10(b)]. CA deposition was recognized on the surface of the bone away from the specimens [Fig. 10(b)].

DISCUSSION

The results from GI-XRD and AES showed that only the CT50 specimen was crystallized to perovskite-type $CaTiO_3$ after the annealing treatment. By annealing in air, the $CaTiO_3$ films were reconstructed, and the crystallinity increased. Simultaneously, Ca in the $CaTiO_3$ film diffused in the direction of the Ti substrate. In CT10, CT20, and CT30 specimens, because of the excessively thin thickness, deficiency of Ca in the $CaTiO_3$ film occurred by Ca diffusion, and the $CaTiO_3$ films were unable to form crystalline $CaTiO_3$. A $CaTiO_3$ film prepared by the RF magnetron sputtering method without any heat treatment reportedly failed to crystallize, and heating over 873 K was required to obtain a crystallized $CaTiO_3$ film.[30,34] Therefore, to obtain a crystallized perovskite-type $CaTiO_3$ thin film, $CaTiO_3$ must be deposited to at least 50 nm in thickness followed by annealing at or above 873 K.

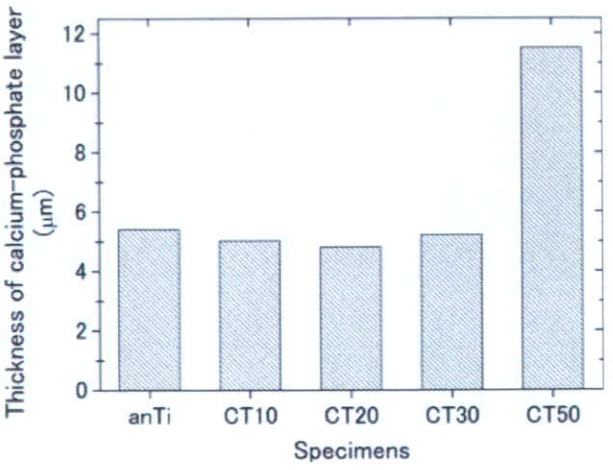

Figure 7. Average of the thickness of the calcium-phosphate layer observed on specimens showing the M4-type surface morphology after 45-days immersion.

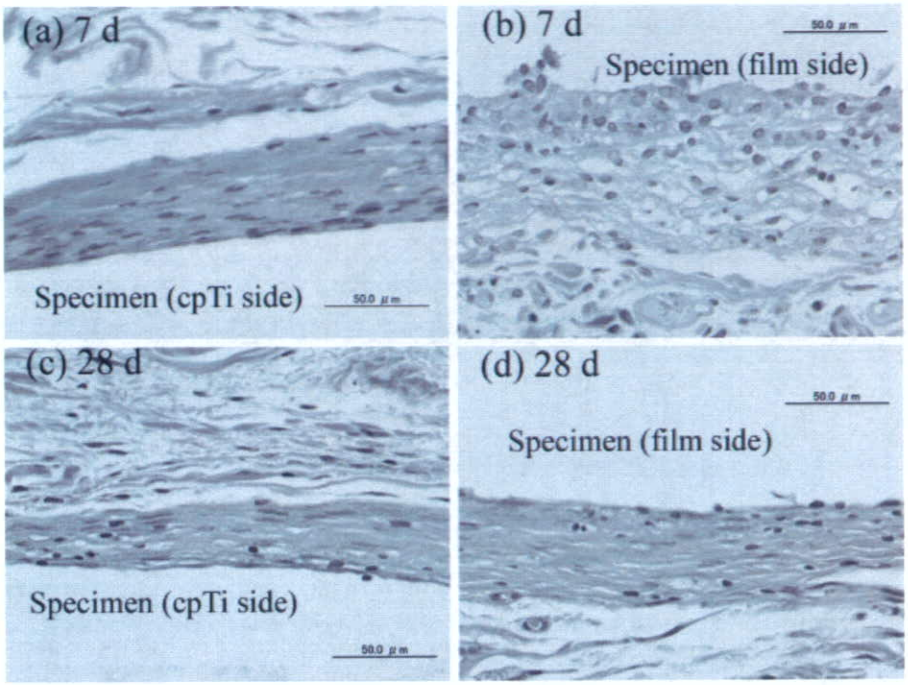

Figure 8. Soft tissue response to specimen in subcutaneous tissue after 7 and 28 days observed by optical microscopy: (a) cpTi side, day 7; (b) $CaTiO_3$ film side, day 28; (c) cpTi side, day 7; (d) $CaTiO_3$ film side, day 28.

The categorization by surface morphologies appears to be related with the nucleation of calcium phosphate. To express the performance of the nucleation of calcium phosphates numerically, a value of the growth degree was assigned to each growing stage observed in Figure 5. Values of 0, 1, 2, and 3 are

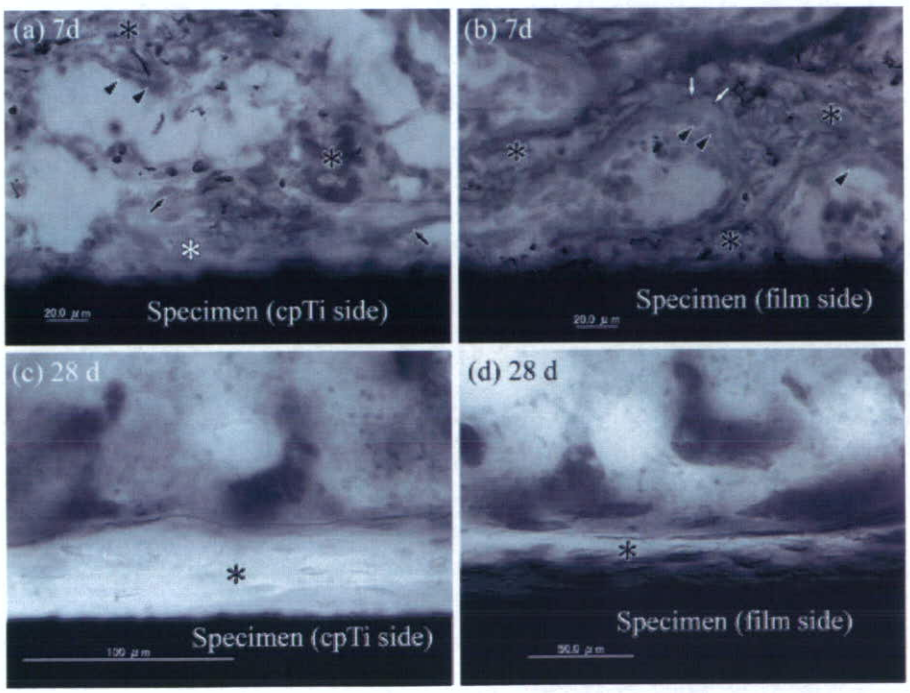

Figure 9. Hard tissue response to the specimen in femoral bone marrow after 7 and 28 days observed by optical microscopy: (a) cpTi side, 7 days; (b) $CaTiO_3$ film side, 7 day; (c) cpTi side, 28 day; (d) $CaTiO_3$ film side, 28 day.

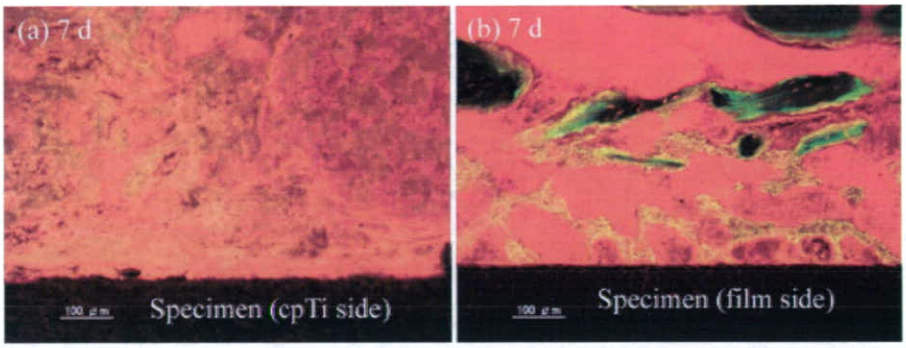

Figure 10. Hard tissue response to the specimen in femoral bone marrow after 7 days observed by fluorescent microscopy: (a) cpTi side; (b) $CaTiO_3$ film side.

assigned to the M1-, M2-, M3-, and M4-stages, respectively. The performance of each specimen was simply expressed by the sum of these values after 35- and 45-days immersion. Thus, the equation is expressed as follows:

$$\text{Performance of the nucleation of calcium phosphates} = \sum_i n_i p_i,$$

where n_i is the number of the i-type morphology and p_i is the value assigned to the i-type morphology. The thickness of the calcium-phosphate layer after immersion appears to be related with the growth rate of calcium phosphate from the nucleus. The thickness of the calcium-phosphate layer after 45-days immersion of each specimen is plotted against the performance of the nucleation of calcium phosphates in Figure 11. A good correlation between the thickness of the calcium-phosphate layer and the performance of the nucleation of calcium phosphates is observed. Judging from Figure 11, the CT50 specimen is clearly superior to the other specimens. Accordingly, it is concluded that a 50-nm $CaTiO_3$ film can enhance the performance most effectively and that 50 nm is the optimum thickness from among all the prepared thicknesses in this study. On the other hand, the performance of $CaTiO_3$ films with thicknesses of 10, 20, and 30 nm was similar to that of the annealed cpTi.

Only the CT50 specimen was crystallized to perovskite-type $CaTiO_3$. It can therefore be concluded that the good performance of the CT50 specimen regarding calcium-phosphate formation is due to this property. On the other hand, since the GI-XRD patterns of CT10, CT20, and CT30 specimens, which contained only Ti and Ti-oxide peaks, were similar to that of the anTi specimen, the calcium included in these specimens was unable to achieve the crystallized phase even after annealing. These results from the surface characterization of CT10, CT20, and CT30 specimens were similar to those of calcium-ion-implanted titanium, which had good performance regarding calcium-phosphate formation.[35] The good calcium-phosphate formation of calcium-ion-implanted titanium was reportedly due to calcium dissolution from the surface.[36] The presence of calcium dissolution from the CT20 specimen shown in Figure 4 is restricted to only the surface area, and the amount of the calcium dissolution would be less than that of calcium-ion-implanted titanium. Thus, it is suspected that calcium in CT10, CT20, and CT30 specimens has no effects on the performance regarding calcium-phosphate formation. Consequently, the performance of CT10, CT20, and CT30 specimens regarding calcium-phosphate formation is similar to that of the anTi specimen.

No severe inflammatory response, such as necrosis and degeneration, was observed on the cpTi side and the $CaTiO_3$ film side, while the tissue reaction around on the cpTi was slighter than that on the $CaTiO_3$ side

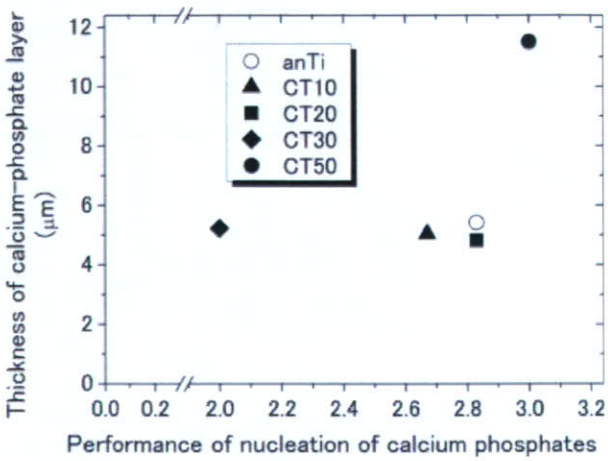

Figure 11. Correlation between the thickness of calcium-phosphate layer after 45-day immersion and the performance of the nucleation of calcium phosphates.

in subcutaneous tissue. However, after 28 days, there was no difference regarding tissue reaction between both sides. The slight inflammatory reaction on the $CaTiO_3$ film side seemed to be caused by the microstructure of the surface. The surface roughness was reported to relate to the tissue reaction.[37] However, these reactions might be bioactive and favorable to osteogenesis on the surface. In bone marrow, active bone formation was recognized on the surface of the $CaTiO_3$ film on day 7, and thinner bone was observed on the $CaTiO_3$ film on day 28. These results suggested that the $CaTiO_3$ film affected osteogenesis within the early stages and that newly formed bone was remodeled on that basis. Active bone formation on the $CaTiO_3$ film at the early implant stage might be related to the calcium phosphate precipitation occurring in HBSS. Osteogenesis on the $CaTiO_3$ film was similar to the bone formation process on HAP-coated and calcium-ion-implanted titanium.[38] These results suggest that $CaTiO_3$-coated titanium has sufficient biocompatibility and potential as a biomaterial.

Therefore, it is concluded that a $CaTiO_3$ coating on titanium could facilitate new bone formation and shorten the bone-fixation term of titanium.

CONCLUSION

A $CaTiO_3$ thin film of 50-nm in thickness deposited on titanium using RF magnetron sputtering followed by annealing at 873 K in air facilitated most effectively the calcium-phosphate formation on titanium in a simulated body fluid. On the other hand, the performance of the $CaTiO_3$ film with a thickness of less than 50 nm was inferior to that of the 50-nm-thick film. Only a 50-nm-thick $CaTiO_3$ film can be crystallized to perovskite-type $CaTiO_3$. The crystallized $CaTiO_3$ coating is required to facilitate effective calcium-phosphate formation on titanium. A $CaTiO_3$ thin film with a thickness of less than 50 nm cannot be crystallized to $CaTiO_3$ by an annealing treatment. The surface properties and performance of these films in HBSS regarding calcium-phosphate formation are similar to those of titanium annealed at 873 K.

No severe inflammatory response to titanium coated with a 50-nm-thick $CaTiO_3$ film was observed in either soft or hard rat tissue. The $CaTiO_3$ coating has sufficient biocompatibility for use as a biomaterial. In hard rat tissue, new bone formation on $CaTiO_3$-coated titanium was more active than that on noncoated titanium, and the bone directly bound to the specimen. The 50-nm-thick $CaTiO_3$ coating is an excellent surface modification method for the facilitation of new bone formation on titanium and can be expected to offer an alternative method to plasma-sprayed HAP.

The authors gratefully acknowledge Mr. Yoshihiro Murakami for operating the EPMA and the Instrument Development Core of the Institute for Materials Research, Tohoku University, for supporting the preparation of specimens.

References

1. Yamamoto A, Honma R, Sumita M. Cytotoxicity evaluation of 43 metal salts using murine fibroblasts and osteoblastic cells. J Biomed Mater Res 1998;39:331–340.
2. Kuroda D, Niinomi M, Morinaga M, Kato Y, Yashiro T. Design, mechanical properties of new β type titanium alloys for implant materials. Mater Sci Eng A 1998;243:244–249.
3. Okazaki Y, Rao S, Tateishi T, Ito Y. Cytocompatibility of various metal and development of new titanium alloys for medical implants. Mater Sci Eng A 1998;243:250–256.
4. Okazaki Y, Rao S, Ito Y, Tateishi T. Corrosion resistance, mechanical properties, corrosion fatigue strength and cytocompatibility of new Ti alloys without Al and V. Biomaterials 1998;13:1197–1215.
5. Speck KM, Fracker AC. Anodic polarization behavior of Ti–Ni and Ti-6Al-4V in simulated physiological solutions. J Dent Res 1980;59:1590–1595.
6. Nakayama Y, Yamamuro T, Kotoura Y, Oka M. In vivo measurement of anodic polarization of orthopedic implant alloys—Comparative-study of in vivo and in vitro experiments. Biomaterials 1989;10:420–424.
7. Okazaki Y, Gotoh E. Comparison of metal release from various metallic biomaterials in vitro. Biomaterials 2005;26: 11–21.
8. De Lange G, De Putter C. Structure of the bone interface to dental implants in vivo. J Oral Implantol 1993;19:123–135.
9. Jasen JA, van der Waerden JP, de Groot K. Development of a new percutaneous access device for implantation in soft tissue. J Biomed Mater Res 1991;25:1535–1545.
10. Denissen HW, de Groot K, Makkes PC, van den Hooff A, Klopper PJ. Tissue response to sense apatite implants in rats. J Biomed Mater Res 1980;14:713–721.
11. Jarcho M. Calcium phosphate ceramics as hard tissue prosthetics. Clin Orthop Relat Res 1981;157:259–278.
12. Tsui YC, Doyle C, Clyne TW. Plasma sprayed hydroxyapatite coatings on titanium substrates, Part 1: Mechanical properties and residual stress levels. Biomaterials 1998;19: 2015–2029.
13. Locardi B, Pazzaglia UE, Gabbi C, Profilo B. Thermal behavior of hydroxyapatite intended for medical applications. Biomaterials 1993;14:437–441.
14. Yamashita K, Yonehara E, Ding X, Nagai M, Umegaki T, Matsuda M. Electrophoretic coating of multilayered apatite composite on alumina ceramics. J Biomed Mater Res 1998;43: 46–53.
15. Yoshinari N, Ohtsuka Y, Derand T. Thin hydroxyapatite coating produced by the ion beam dynamic mixing method. Biomaterials 1994;15:529–535.
16. Ong JL, Lucas LC. Post-deposition heat treatments for ion beam sputter deposited calcium phosphate coatings. Biomaterials 1994;15:337–341.
17. van Dijk K, Schaeken HG, Wolke JGG, Jansen JA. Influence of annealing temperature on RF magnetron sputtered calcium phosphate coatings. Biomaterials 1996;17:405–410.
18. De Groot K, Geesink R, Klein CP, Serekian P. Plasma sprayed coatings of hydroxylapatite. J Biomed Mater Res 1987;21: 1375–1381.
19. Lin JHC, Liu ML, Ju CP. Structure and properties of hydroxyapatite–bioactive glass composites plasma sprayed on Ti-6Al-4V. J Mater Sci Mater Med 1994;5:279–283.

20. Brossa F, Cigada A, Chiesa R, Paracchini L, Consonni C. Adhesion properties of plasma sprayed hydroxyapatite coatings for orthopaedic prostheses. Biomed Mater Eng 1993;3:127–136.
21. Inadome T, Hayashi K, Nakashima Y, Tsumura H, Sugioka Y. Comparison of bone-implant interface shear strength of hydroxyapatite-coated and alumina-coated metal implants. J Biomed Mater Res 1995;29:19–24.
22. Hayashi K, Inadome T, Tsumura H, Nakashima Y, Sugioka Y. Effect of surface roughness of hydroxyapatite-coated titanium on the bone-implant interface shear strength. Biomaterials 1994;15:1187–1191.
23. Geesink RGT, de Groot K, Klein CP. Bonding of bone to apatite-coated implants. J Bone Joint Surg Br 1988;70:17–22.
24. Radin SR, Ducheyne P. Plasma spraying induced changes of calcium phosphate ceramic characteristics and the effect on in vitro stability. J Mater Sci Mater Med 1992;3: 33–42.
25. Ducheyne P, Radin S, King L. The effect of calcium phosphate ceramic composition and structure on in vitro behavior. I. Dissolution. J Biomed Mater Res 1993;27:25–34.
26. Ong JL, Lucas LC. Post-deposition heat treatment for ion beam sputter deposited calcium phosphate coatings. Biomaterials 1992;15:337–341.
27. Yoshinari M, Ohtsuka Y, Derand T. Thin hydroxyapatite coating produced by the ion beam dynamic mixing method. Biomaterials 1994;15:529–535.
28. de Groot K, Geesink R, Klein CPA, Serekian P. Plasma sprayed coating of hydroxylapatite. J Biomed Mater Res 1987;21: 1375–1381.
29. Geesink RGT, de Groot K, Klein CPAT. Chemical implant fixation using hydroxyl-apatite coatings. The development of a human total hip prosthesis for chemical fixation to bone using hydroxyl-apatite coatings on titanium substrates. Clin Orthop Relat Res 1987;225:147–170.
30. Ohtsu N, Sato K, Saito K, Asami K, Hanawa T. Calcium phosphates formation on $CaTiO_3$ coated titanium. J Mater Sci Mater Med. Forthcoming.
31. Ohtsu N, Sato K, Saito K, Hanawa T, Asami K. Evaluation of degradability of $CaTiO_3$ thin film in simulated body fluids. Mater Trans 2004;45:1778–1781.
32. Ohtsu N, Ashino T, Asami K. Silicon contamination adsorbed o pure titanium plate during soaking test in Hanks' balanced saline solution. Mater Trans 2004;45:550–553.
33. Yokoyama A, Matsumoto H, Yamamoto S, Kawasaki T, Kohgo T, Uo M, Watari F, Nakasu M. Tissue response to a newly developed calcium phosphate cement containing succinic acid and carboxymethyl–chitin. J Biomed Mater Res A 2003;64:491–501.
34. Ohtsu N, Saito K, Asami K, Hanawa T. Characterization of $CaTiO_3$ thin film prepared by ion-beam assisted deposition. Surf Coat Technol 2006;200:5455–5461.
35. Hanawa T, Murakami K, Kihara S. Calcium Phosphate Precipitation on Calcium-Ion-Implanted Titanium in Electrolyte. In: Horowitz E, Parr JE, editors. Characterization and Performance of Calcium Phosphate Coatings for Implant. Philadelphia: American Society for Testing and Materials; 1994. p 170. ASTM STP 1196.
36. Hanawa T, Asami K, Asaoka K. Microdissolution of calcium ions from calcium-ion-implanted titanium. Corros Sci 1996;38: 1579–1594.
37. Parker J, Walboomers X, Von den Hoff J, Maltha J. Soft-tissue response to silicone and poly-L-lactic acid implants with a periodic or random surface micropattern. J Biomed Mater Res 2002;61:91–98.
38. Hanawa T, Kamiura Y, Yamamoto S, Kohgo T, Amemiya A, Ukai H, Murakami K, Asaoka K. Early bone formation around calcium ion implanted titanium inserted into rat tibia. J Biomed Mater Res 1997;36:131–136.

Materials Science Forum Vols. 539-543 (2007) pp. 563-566
online at http://www.scientific.net

Biofunctional Hybrid of Titanium with Polymers

Takao Hanawa[a], Harumi Sakamoto[b] and Yuta Tanaka[c]

Department of Metallurgy, Institute of Biomaterials and Bioengineering, Tokyo Medical and Dental University, 2-3-10 Kanda-surugadai, Chiyoda-ku, Tokyo 101-0062, Japan

[a] hanawa.met@tmd.ac.jp, [b] sak-met@tmd.ac.jp, [c] y_tanaka_r@mail.goo.ne.jp

Keywords: titanium, polymer, PEG, segmentated polyurethane, immobilization, electrodeposition, silane coupling.

Abstract. Application of metals will be expanded to new medical devices, scaffold for tissue engineering, artificial organs, etc. with the addition of biofunction. Therefore, immobilization or combination of functional polymers to metals is significant subject for the application of metals to biofunctional materials and sensors. Metal-polymer hybrid materials are promising biomaterials future, especially for artificial organs. To form metal-polymer hybrid for biomedical devices, two techniques are predominant according to the purpose: Immobilization of biofunctional polymers to metals and bonding of biopolymers with metals. In the first case, poly(ethylene glycol: PEG) is a biofuctional molecule on which adsorption of proteins is inhibited. Control of immobilization mode of PEG modified with NH_2 to titanium surface by electrodeposition is feasible and the adsorption of proteins is inhibited by the deposited PEG. This technique could be applied to all metallic materials. In the other case, we attempted to form a composite of titanium with segmentated polyurethane (SPU) thorough silane-coupling agent (γ-MPS). This composite material is applied to texture of titanium covered by SPU as artificial organs.

Metals as Biomaterials

Metals are used as biomaterials and over 70% of implant devices consist of metals. Advantages of metals are large strength and toughness in comparison with ceramics and polymers. However, metals are sometimes misunderstood as unfavorite materials for medical use that show toxicity, fatigue, and corrosion in the human body (Fig. 1). In addition, metals themselves never show biofunction because no biofunction is added to metals during manufacturing process: melting, casting, fogging, rolling, and heat treatment. Therefore, metals are not expected as biofunctional materials. In order to add a biofunction to metals, surface modification is absolutely necessary.

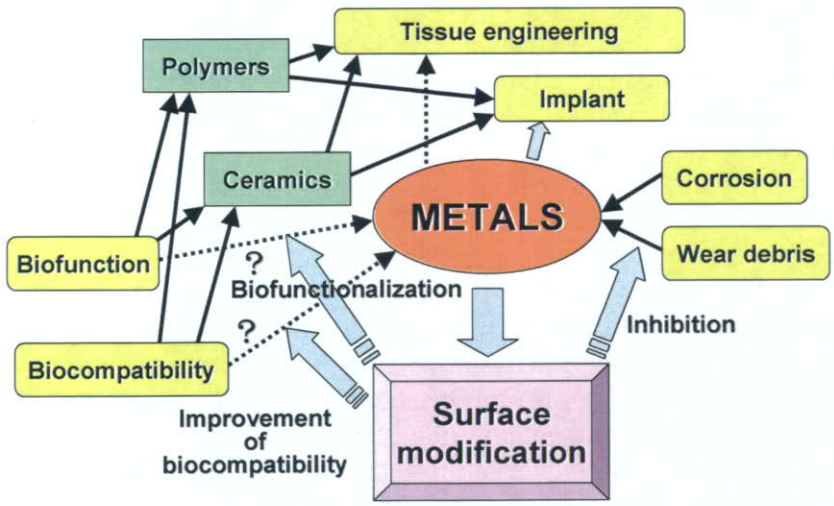

Fig. 1. Situation of metals as biomaterials and surface modification.

Following applications of metals are expected as biomaterals:

1. Implant for orthopedics, cardiovascular surgery, and dentistry.
   Bone formation, soft tissue adhesion, and blood compatibility are requested.
2. Scaffold materials for tissue engineering.
   Cell adhesion and activation of cells are requested.
3. Base materials for biosensing.

Inhibition of cell adhesion and biomolecule adsorption is requested.
For these applications, controlling of cell adhesion and protein adsorption is the most important event.

When a metallic material is implanted into a human body, immediate reaction occurs between its surface and the living tissues. In other words, immediate reaction at this initial stage straightaway determines and defines a metallic material's tissue compatibility. Since conventional metallic biomaterials are usually covered with metal oxides, surface oxide films on metallic materials play an important role not only against corrosion but also in tissue compatibility. Surface properties of a metallic material may be controlled with surface modification techniques.

Surface Modification

Surface properties of a metallic material may be controlled with surface modification techniques. To develop and apply the appropriate surface modification technique, knowledge of the material's surface composition is absolutely necessary. This is because surface modification is a process that improves surface property by changing the composition and structure, while leaving the mechanical properties of the material intact. Surface modification is a process that changes a material's surface composition, structure and morphology, leaving the bulk mechanical properties intact. With surface modification, chemical and mechanical durability, as well as tissue compatibility of surface layer could be improved. Surface property is particularly significant for biomaterials, and thus surface modification techniques are particularly useful to biomaterials. Dry-process (using ion beam) and hydro-process (which is performed in aqueous solutions) are predominant surface modification techniques. Apatite coating on titanium with plasma spray, titanium nitride coating with sputter deposition, and titanium oxide growth with morphological control by electrolysis are already available for commercial use (as shown in Fig. 2).

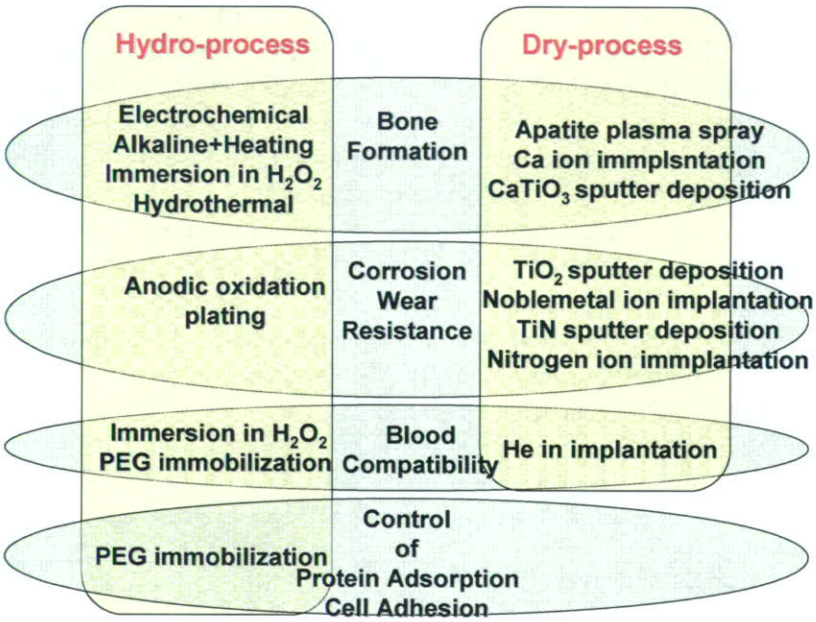

Fig. 2. Surface modification of metals as biomaterials.

Metal-Polymer Composite

Polymers sometimes show a lack of strength and durability as a biomaterial. On the other hand, metals are used because of their high durability, strength, and formability, while they do not have bioactive and biofunctional properties. Metal-polymer hybrid materials are promising biomaterials future, especially for artificial organs.

In the design of bone-substituting and blood-contacting materials for both medical implants and bioaffinity sensors, it is a major challenge to generate surfaces and interfaces that are able to withstand proteins adsorption.

To accelerate bone formation surrounding implant materials, the materials are modified with biomolecules. Several phospholic acids were synthesized and grafted onto titanium. Proliferation, differentiation and protein production of rats' osteoblastic cells on the titanium were then

investigated [1]. Type I collagen production increased with modification by ethane-1,1,2-triphospholic acid and methylenediphosphonic acid. To improve hard tissue response, bone morphogenetic protein-4 (BMP-4) was immobilized on Ti-6Al-4V alloy through lysozyme [2]. To improve tissue compatibility, attempts were made for silane chemistry to couple proteins to the oxidized metal surfaces of Co-Cr-Mo, Ti-6Al-4V, Ti and Ni-Ti [3].

Platelets adhesion, adsorption of proteins, peptides and antibodies, and DNA can likewise be controlled by modifications. A class of copolymers based on poly (L-lysine)-g-poly (ethylene glycol), PLL-g-PEG, was found to spontaneously adsorb from aqueous solutions onto TiO_2, $Si_{0.4}Ti_{0.6}O_2$ and Nb_2O_5 to develop blood-contacting materials and biosensors [4]. Poly(ethylene glycol)-poly(DL-lactic acid) (PEG-PLA) copolymeric micelles were attached on functionalized TiO_2 and Au. The micelle layer enhanced the protein resistance of the surfaces by up to 70%.

Silicon and titanium oxide surfaces (SiO_2/Si and TiO_2/Ti) were covalently modified with bioactive molecules (*e.g.*, peptides) in a simple three-step procedure to control cellular and biomolecular functions on the surfaces. Bioactive surfaces were synthesized by first immobilizing N-(2-aminoethyl)-3-aminopropyl-trimethoxysilane (EDS) to polished quartz disks, polished silicon wafers or sputter-deposited titanium films. Subsequently, a maleimide-activated surface — amenable to tethering molecules — with a free thiol (e.g., cysteine) was created by coupling sulfosuccinimidyl 4-(N-maleimidomethyl) cyclohexane-1-carboxylate (sulfro-SMCC) to the terminal amine on EDS. Peptides with terminal cysteine residues were immobilized on maleimide-activated oxides [5].

The surface of stainless steel was first modified by the silane coupling agent (SCA), (3-mercaptopropyl)trimethoxysilane. The silanized stainless steel surface (SCA-SS surface) was subsequently activated by argon plasma and then subjected to UV-induced graft polymerization of poly(ethylene glycol)methacrylate (PEGMA). The PEGMA graft-polymerized stainless steel coupon (PEGMA-g-SCA-SS) with a high graft concentration, and thus a high PEG content, was found to be very effective in preventing bovine serum albumin and γ-globulin adsorption [6].

Metal oxide surfaces (Ta_2O_5, Al_2O_3, Nb_2O_5, ZrO_2, SiO_2) were coated by self-assembled monolayers (SAMs) of dodecyl phosphate ($DDPO_4$) and 12-hydroxy dodecyl phosphate ($OH\text{-}DDPO_4$). The coating was done by a novel surface modification protocol based on the adsorption of alkyl phosphate ammonium salts from aqueous solution for application to biochemical analyses and biosensors [7]. To apply a surface plasmon resonance (SPR) to biosensors, a sandwich immunoassay was performed on a thin gold film set in SPR cell. The molecular motion of self-assembled monolayers on gold was examined using SPR under an electric field.

To form metal-polymer hybrid for biomedical devices, two techniques are predominant according to the purpose: Immobilization of biofunctional polymers to metals and bonding of biopolymers with metals.

Immobilization of Biofunctional Polymers to Metals

In the first case, poly(ethylene glycol), PEG, is a biofuctional molecule on which adsorption of proteins is inhibited. In stents, blood compatibility or prevention of adhesion of platelet is necessary. In guide wires and guiding cathetels, sliding lubrication in blood vessel is important when those are inserted into there. For these purpose, the fundamental property required to metal surface is the inhibition of protein adsorption. PEG is a unique biofuctional molecule on which adsorption of proteins is inhibited. No universal and one-stage technique for the immobilization of PEG to base metals has been developed. In this study, PEG terminated at both terminals or one terminal with amine bases was immobilized onto titanium surface with electrodeposition. The PEG was solved to NaCl solution and electrodepsition was carried out in the electrolyte with 5 V for 300 s. The thickness of deposited PEG layer was determined using ellipsometry and bonding manner of PEG to titanium surface was characterized using X-ray photoelectron spectroscopy (XPS). As a result, a certain

amount of PEG is adsorbed on titanium not only with electrodeposition but also with immersion when PEG is terminated by amine. However, terminated amines exist at the surface of titanium and combines with titanium oxide as N-HO by electrodeposition, while amines randomly exist in the deposited layer and show ionic bond with titanium oxide by immersion. Moreover, the difference in amine termination leads to different bonding manner, U-shape in PEG terminated both terminals and brush in PEG terminated one terminal. Electrodeposition of PEG was effective for the inhibition of the adsorption of albumin. This process is useful for all electroconductive materials and complicated morphology [8].

Combination of Metals with Biopolymers

On the other hand, to develop metal-polymer complexes with high mechanical strength and flexibility for implants, Ti combined with a segmentated polyurethane (SPU) through a 3-(trimethoxysilyl) propylmethacrylate (γ-MPS) as a coupling agent in this study (Fig. 3). The effects of thickness of γ-MPS layer and polymerization on the tensile and shear strengths of Ti-SPU bonding were evaluated. The thickness of γ-MPS layer was determined by an ellipsometer. The failure interface was characterized using scanning electron microscopy and bonding manner were characterized using XPS and glow discharge optical emission spectrometry (GD-EOS). Consequently, the thickness of γ-MPS layer increased with the increase of the solution concentration of γ-MPS and soaking time. Bonding strength between Ti and SPU was dramatically increased in the presence of γ-MPS layer and increased with the thickness of the layer. Failure inside γ-MPS layer was found when the γ -MPS thickness was 1 nm, while failure in γ -MPS/SPU interface and SPU cohesion failure were observed when the γ -MPS thickness was more than 1 nm. Furthermore, after soaking in Hanks' solution at 310 K for 1 month, the tensile and shear strength of Ti-SPU bonding were slightly decreased. On the other hand, they increased with ultraviolet ray radiation and/or heating. This study revealed the useful of γ-MPS to improve between Ti and SPU for implants. This Ti-SPU composite may be a future promising biomaterial.

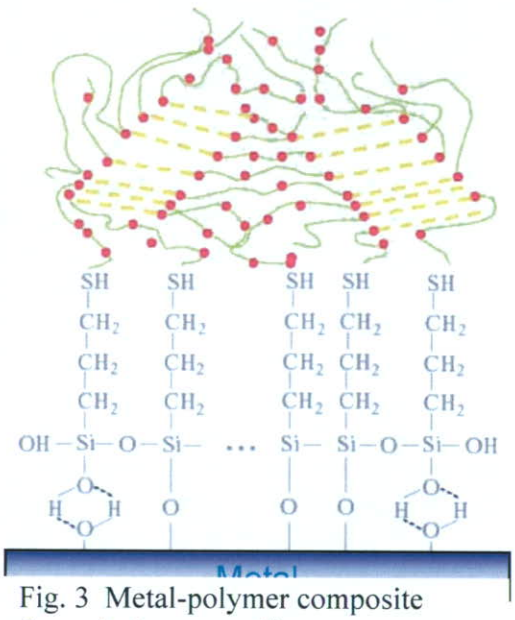

Fig. 3 Metal-polymer composite through sirane coupling

References

[1] C. Viornery, H. L. Guenther, B.-O. Arronson, P. Pechy, P. Descouts and M. Gratzel: J. Biomed. Mater. Res. Vol. 62 (2002), p.149.
[2] D. A. Puleo, R. A. Kissling and M.-S. Sheu: Biomaterials Vol. 23 (2002), p.2079.
[3] A. Nanci, J. D. Wuest, L. Peru, P. Brunet, V. Sharma, S. Zalzal and M. D. McKee: J. Biomed. Mater. Res. Vol. 40 (1998), p.324.
[4] N. P. Huang, R. Michel, J. Vörös, M. Textor, R. Hofer, A. Rossi, D. L. Dlbert, J. A. Hubbell and N. D. Spencer: Langmuir Vol. 17 (2001), p.489.
[5] S. J. Xiao, M. Textor, N. D. Spencer and H. Sigrist: Langmuir Vol. 114 (1998), p.5507.
[6] F. Zhang, E. T. Kang, K. G. Neoh, P. Wang and K. L. Tan: Biomaterials Vol. 22 (2001), p. 1541.
[7] M. Textor, L. Ruiz, R. Hofer, A. Rossi, K. Feldman, G. Hähner and N. D. Spencer: Langmuir Vol. 16 (2000), p. 3257.
[8] Y. Tanaka, H. Doi, Y. Iwasaki, S. Hiromoto, T. Yoneyama, K. Asami, H. Imai and T. Hanawa: Mater. Sci. Eng. C (in press).

Advanced Materials Research Vols. 15-17 (2007) pp. 205-208
online at http://www.scientific.net

Immobilization of Poly(Ethylene Glycol) Terminated with Amine to Titanium Surface by Electrodeposition

Y.Tanaka, H.Doi, Y.Iwasaki, T.Yoneyama and T.Hanawa

Institute of Biomaterials and Bioengineering, Tokyo Medical and Dental University

2-3-10 Kanda-Surugadai, Chiyoda-ku, Tokyo 101-0062, Japan

[a] y_tanaka_r@mail.goo.ne.jp, [b] doi.met@tmd.ac.jp, [c] yasu.org@tmd.ac.jp,

[d] yoneyama.met@tmd.ac.jp, [e] hanawa.met@tmd.ac.jp

Keywords: Titanium, Poly(ethylene glycol), Immobilization, Electrodeposition, Surface analysis

Abstract. In many applications such as catheters, artificial blood vessels and diagnostic sensors, blood compatibility or prevention of adhesion of platelet is required. The preferred way to control these purposes is to eliminate or drastically reduce the adsorption of proteins. Surface modification with Poly(ethylene glycol), PEG has long been known to reduce undesirable protein adsorption. No technique for the immobilization of PEG to base metal has been developed. In this study, PEG terminated at both terminals or one terminal with amine bases was immobilized onto titanium surface by immersion or electrodeposition. The bonding manners of PEG onto titanium, which involve directionality of terminated amines and chemical bonding states of interface between the deposited PEG layer and TiO_2, were characterized using X-ray photoelectron spectroscopy, XPS. As a result, terminated amines locate inside of the PEG layer and combine mainly with TiO_2 as stable NHO by electrodeposition, while amines randomly exist and show mainly unstable bonding with TiO_2 by immersion. Moreover, the difference of amine termination leads to different bonding manners, U-shape in PEG terminated both terminals and brush in PEG terminated one terminal. This immobilization process is one-stage convenient technique and useful for all electroconductive and morphological materials.

Introduction

Metals are often applied in medical and dental devices because they have greater strength and toughness than ceramics or polymers. Therefore, metals cannot be replaced with ceramics or polymers at present. On the other hand, metallic materials are generally not expected to be the biomaterials of the future at the research level because they do not have bioactive and biofunctional properties. However, metals with biofunctions have been required in the recent past. For example, in the area of blood-contacting devices such as stents and catheters, preventing the adsorption of proteins and platelets, blood activation and thrombus formation is required. In guide wires and guiding cathetels, lubrication in the blood vessels is also important for proper sliding and insertion. Surface modification using biofuctional molecule such as heparin, self-assembled monolayer and poly(ethylene glycol), PEG has been shown to be effective for these purposes. Of these, PEG continues to provide the most promising results in terms of reducing undesirable protein adsorption. Therefore, the immobilization of PEG to a metal surface is an important method towards the biofunctionalization of the metal surface.

The immobilization of biofuctional polymers on a noble metals such as gold is usually conducted by –SH or –SS– binding; however, this technique can only be used for noble metals. In addition, a polycationic comb-like graft co-polymer, poly (L-lysine)-*g*-poly (ethylene glycol), PLL-*g*-PEG, is immobilized onto negatively charged metal oxide surfaces by a dipping process into an aqueous solution of the polymer. A surface of stainless steel was firstly modified by a silane-coupling agent, SCA, (3-mercaptopropyl)trimethoxysilane. These processes require several stages but are effective for immobilization; however, no promising technique for the immobilization of PEG to a metal surface has been so far developed.

In this study, PEG terminated at both terminals or one terminal with amine bases was immobilized onto a titanium surface by immersion or electrodeposition in an attempt to develop a new technique that could be used for all metals and morphological materials. Furthermore, directionality of terminated amines and chemical bonding states of interface between the deposited PEG layer and TiO_2 were characterized using X-ray photoelectron spectroscopy, XPS because the protein-repellent effects or durability of PEG layer could be controlled by the bonding manners of PEG onto titanium surface. Finally, the adsorption of albumin on the PEG immobilized surface formed by immersion or electrodeposition was evaluated.

Experimental procedure

Both terminals of PEG were terminated with amine (B-PEG; PEG1000 Diamine, NOF Corporation, Japan), and only one terminal was terminated with amine (O-PEG; SUNBRIGHT MEPA-10H, NOF Corporation, Japan) because the terminals of PEG is positively charged, from NH_2 to NH_3^+, for electrodeposition. The chemical structures of the PEGs are shown in Fig. 1. Molecular weights of both PEGs were about 1000. 2mass% PEG was dissolved in a 0.3 mol L^{-1} NaCl solution, and electrodeposition was carried out at 310 K with –5 V for 300 s (Fig. 2). The pH of the solution with PEG was 11. Therefore, titanium oxide surface is negatively charged. A commercially pure titanium disk (diameter 8 mm , thickness 2 mm) with grade 2 was metallographically polished and ultrasonically rinsed in acetone and deionized water. The titanium disk was fixed in a polytetrafluoroethylene holder that exposed the area of 28.3 mm^2. The cathodic potential was charged from open circuit potential, E_{open} to –5 V vs. SCE and maintained at this potential for 300 s. For comparison, titanium was immersed in the electrolyte containing B-PEG for 2 h and 24 h without any electric charge at 310 K.

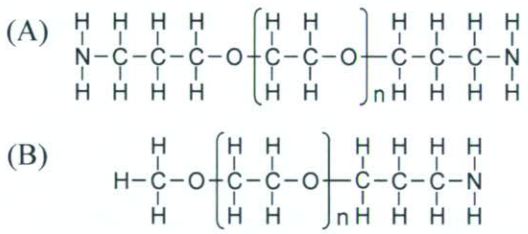

Fig. 1. Chemical structures of PEGs in which both terminals (A) and one terminal (B) were terminated with amine.

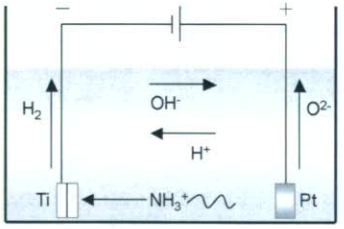

Fig. 2. Schematic illustration of electrodeposition.

The thickness of the PEG layer deposited on titanium surface was determined with an ellipsometer (DVA-36Ls, Mizojiri Optical Co., Ltd.) in air. The bonding manners of PEG onto titanium were characterized using XPS (SSI-SSX100). The take-off angle for photoelectron detection was 35° from the surface of the specimen. The inhibition of protein adsorption to a PEG immobilized surface was evaluated. Albumin (fluorescein isothiocyanate conjugated bovine, A9771, Sigma) was dissolved into phosphate-buffered saline without calcium chloride and magnesium chloride (PBS: Dulbecco's PBS, D1408, Sigma) with a concentration of 4.5 g L^{-1}. The PEG immobilized specimens were immersed in albumin-containing PBS for 30 min, rinsed with PBS and deionized water, and then dried with a stream of nitrogen gas (99.9%). The surface of specimens was observed with a fluorescence microscope (E-600, Nikon).

Results and discussion

Fig. 3 shows the thicknesses of the PEG layers determined by ellipsometry. These thicknesses are measured in air; therefore, the real thickness in solutions is larger than these values because the PEG layers swell on exposure to water. The thickness of the PEG layer, which is the amount of

immobilized PEG, was the largest in this order: 24 h immersion in B-PEG, electrodeposition of B-PEG for 300 s, electrodeposition of O-PEG for 300 s, and 2h immersion in B-PEG. This indicated that electrodeposition was more effective than immersion for the immobilization of PEG on the titanium surface. In case of 24 h immersion in B-PEG, the charged terminals of PEG attracted electrostatically titanium surface.

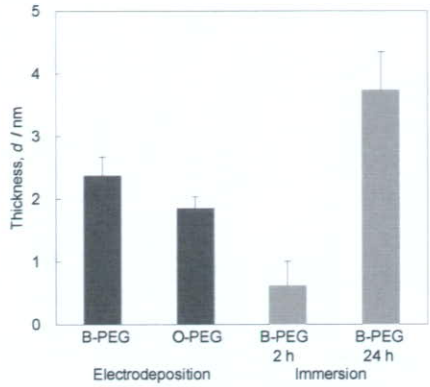

Fig. 3 Thickness of the PEG layer deposited on titanium by electrodeposition and immersion. B-PEG: both-terminal-modified PEG. O-PEG: one-terminal-modified PEG.

Carbon, nitrogen, oxygen, and titanium were detected using XPS and typical XPS spectra of C 1 and N 1s electron energy regions of these elements are shown in Fig. 4. Integrated intensities of these elemental peaks are originated from their own chemical states shown in Fig. 4 [1-3]. The proportion of the integrated intensity equals to that of existence.

The change in the ratios, [C-O, C-N]/[C-C, CH_2], in the C 1s peak in each specimen is shown in Fig. 5. The C-N bond governs this ratio because C-C bonds exist in the entire molecule of PEG, while C-N bonds only exist in the terminals. The photoelectron signals in XPS abruptly decay depending on the depth direction. Therefore, the C-N bond at terminals was located inside of the PEG layer by electrodeposition more often than by immersion. In other words, nitrogen atoms were located at the interface between PEG and TiO_2 by electrodeposition.

The change in the ratios, [NH_3^+]/[NHO], in the N 1s peak is shown in Fig. 6. This ratio was much smaller in electrodeposited specimens than in immersed specimens. Therefore, amines in terminals existed mainly as stable NHO bond rather than as unstable NH_3^+ by electrodeposition.

These XPS results are illustrated the PEG immobilized manners onto titanium surfaces as Fig. 7. Amines in terminals locate inside of the PEG layer and combine mainly with TiO_2 as stable NHO by electrodeposition, while amines randomly exist and show mainly unstable bonding with TiO_2 by immersion. Also, the difference of amine termination leads to different bonding manners, U-shape in B-PEG and brush in O-PEG. This immobilization process is one-stage convenient technique and useful for all electroconductive and morphological materials. Moreover, the electrodeposition of PEG was effective for the inhibition of albumin adsorption.

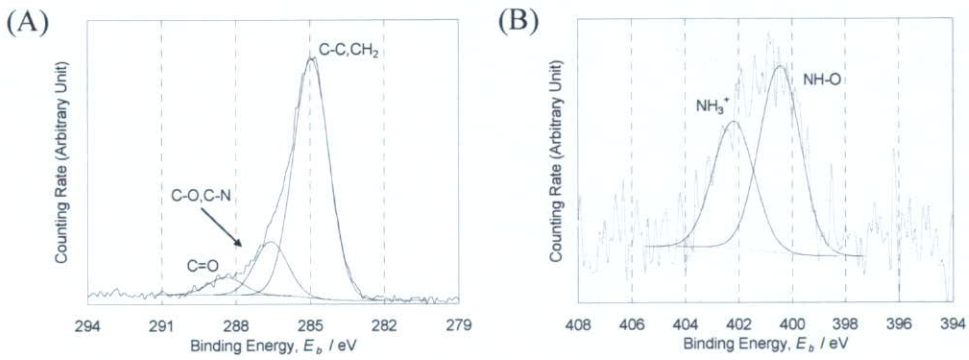

Fig. 4. C 1s (A) and N 1s (B) electron energy region spectra by XPS and decomvolution of the peaks to component peaks.

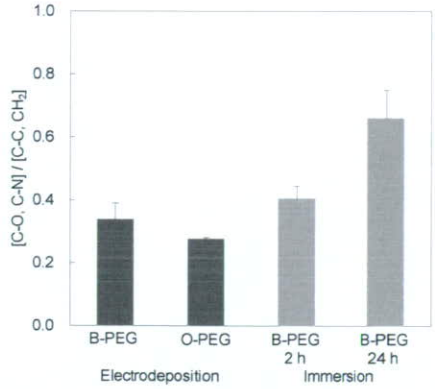

Fig. 5. Ratio, [C-O,C-N] / [C-C,CH], obtained from the deconvoluted C 1s electron energy region peak. B-PEG: both-terminal-modified PEG. O-PEG: one-terminal-modified PEG.

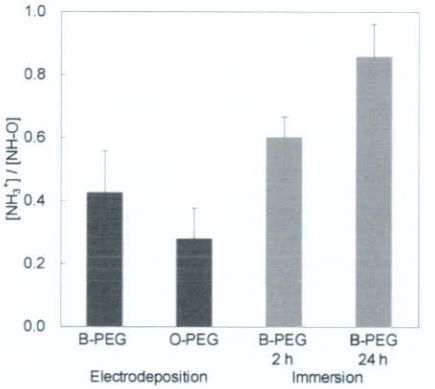

Fig. 6. Ratio, $[NH_3^+]/[NHO]$, obtained from the deconvoluted N 1s electron energy region peak. B-PEG: both-terminal-modified PEG. O-PEG: one-terminal-modified PEG.

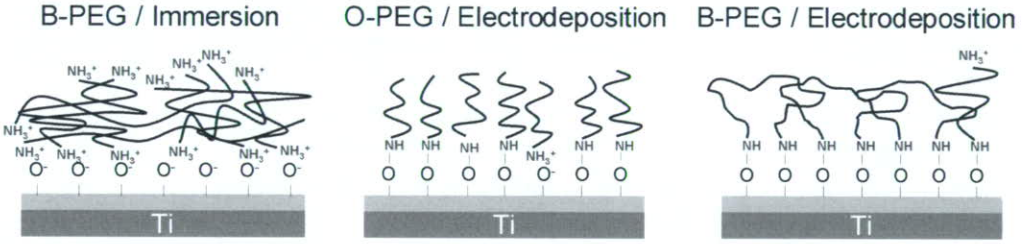

Fig. 7. Schematic model of the deposition mode and chemical bonding state of PEG by immersion and electrodeposition.

Conclusions

A certain amount of PEG was adsorbed on titanium by both electrodeposition and immersion when PEG is only terminated by amine. However, terminated amines exist at the surface of titanium and are combined with TiO_2 as stable NHO by electrodeposition, while amines randomly exist and show an unstable bonding with TiO_2 by immersion. The B- PEG is immobilized as a U-shape, and the O-PEG is immobilized as a brush. The electrodeposition of PEG was effective for the inhibition of albumin adsorption. This immobilization process is useful for all electroconductive and morphological materials.

References

[1] T. Hanawa, K. Asami, K. Asaoka, J. Biomed. Mater. Res. Vol. 40 (1998), p.530-538.

[2] B. Lindberg, R. Maripuu, K. Siegbahn, R. Larsson, C.-G. Gölander, J. C. Eriksson, J. Colloid Interf. Sci. Vol. 95 (1983), p.308-321.

[3] T. Solomun, A. Schimanski, H. Sturm, E. Illenberger, Chem. Phys. Lett. Vol. 387 (2004), p.312-316.

Advanced Materials Research Vols. 15-17 (2007) pp. 125-128
online at http://www.scientific.net

A New Technique of Titanium and Segmented Polyurethane Complex through 3-(trimethoxysilyl) propylmethacrylate for Artificial Implants

Harumi Sakamoto [a], Hisashi Doi [b], Equo Kobayashi [c] and Takao Hanawa [d]

Institute of Biomaterials and Bioengineering, Tokyo Medical and Dental University, Tokyo 101-0062, Japan

[a]sak-met@tmd.ac.jp, [b]doi.met@tmd.ac.jp, [c]equo.met@tmd.ac.jp, [d]hanawa.met@tmd.ac.jp

Keywords: Titanium, Segmented polyurethane, Silane coupling agent, Shear stress, Surface analysis.

Abstract. To develop metal-polymer composite with high mechanical strength and flexibility for artificial implants, commercially pure titanium (Ti) combined with segmented polyurethane (SPU) through (3-trimethoxysilyl) propylmethacrylate (γ-MPS). The effects of thickness of γ-MPS layer on the shear bonding strength between Ti and SPU were investigated. The thickness of γ-MPS layer was determined by ellipometry. Shear bonding stress of Ti-SPU composite was measured by shear bonding test. Furthermore, fractured surface of Ti-SPU composite was analyzed by optical microscopy and X-ray photoelectron spectroscopy. Consequently, shear bonding stress of Ti-SPU composite was dramatically increased with the increase of the γ-MPS layer thickness. This study revealed that γ-MPS is useful to improve bonding between Ti and SPU for artificial implants.

Introduction

Currently, polymers are widely used as biomaterials because of their multiple functions. In particular, biofunctionalizations by surface modification to polymer surface are important to achieve improvement of biocompatibility. However, polymers sometimes show insufficient strength and durability for some purpose caused from their structure. On the other hand, metals are widely used as biomaterials like stents, hip joints and bone plates with a long history, since metals have good mechanical properties, especially toughness, and long terms durability. If once polymer and metal were bonded and used as a composite material, a new material having good biocompatibility and high mechanical strength could be created. It is required that interfacial structure designing of composite to develop the material that function based on the structure at nanometer level.

In the dental field, bonding of polymer with metal has been required to make dentures till today. In particular, silane coupling agent which has difunctional molecules is widely used to combine metal and polymer. However, most of research on bonding with silane coupling agent in the dental material field were only investigated about bonding force, and there is few report that examines which factors of the silane coupling agent influences the bonding.

The aim of this study is to establish the technique of metal-polymer composite using silane coupling agent and to investigate accurate appraisal methods of these composites. As the base materials for the composite, titanium (Ti) and segmented polyurethane (SPU) were employed. Titanium is the most promising metallic biomaterial and segmented polyurethane is also widely used because of its antithrombogenicity. Shear bonding force between Ti and SPU that were made in various conditions was measured by shear bonding test. Furthermore, structure at nanometer level of fractured surface of composite after shear bonding test was investigated by X-ray photoelectron spectroscopy (XPS). From these experimental, factors that affect on bonding were specified.

Material and Methods

Grade 2 commercially pure titanium (CP-Ti) disks with 2 and 5 mm in thickness and 8

mm in diameter were prepared from wrought titanium rods (Rare Metallic Co., Inc., Japan). The disks were metallographically polished and ultrasonically rinsed in acetone and deionized water. 0.1, 0.5, 1.0, 2.0 vol.% (3-mercaptopropyl)trimethoxysilane (γ-MPS) solutions were prepared by diluting 100% concentration of γ-MPS (Kanto Chemical Co., Inc., Japan) with deionized water which adjusted pH 4 using acetic acid. The disks were then immersed in the freshly prepared γ-MPS solution for 1, 10, 50 and 100 min. 2-mm thick disk coated with γ-MPS was used for the determination of the thickness of γ-MPS layer by ellisometry, whereas 5-mm thick disks were continually used for shear bonding test. 3% SPU was prepared from a mixture of 600 mg Corehtane70A (Crovita, USA), 10 mL tetrahydrofuran (Kanto Chemical Co., Inc., Japan) and 10 mL dimethylformamide (Kanto Chemical Co., Inc., Japan). 5-mm thick disks coated with γ-MPS were then immersed in the freshly prepared SPU solution and kept in a vacuum desiccator for 2 days. Then titanium-SPU (Ti-SPU) composite grip was made by bonding autopolymerized acrylic resin (UNIFAST II, GC, Japan) to SPU coated 5-mm thick disks, which were used in the shear bonding test.

Thickness of γ-MPS layer was determined using elliposometry (DVA-36Ls, Mizojiri Optical Co., Ltd., Japan) in air. Light source was He-Ne laser (632.8 nm) and the incident angle to the titanium surface was 70°. The thickness was calculated by optical constants of the refractive index and absorption coefficient of titanium oxide on the titanium substrate, 2.209 and 3.079, respectively.

Shear bond strength of the Ti-SPU composite was evaluated using an universal mechanical test machine (2000-IB, Shimadzu, Japan) with a crosshead speed of 0.1 mm s^{-1} at room temperature. For the shear bonding test, an apparatus was originally designed as shown in Fig.1. The SPU fractured area was measured using a personal computer (NIH Image 1.62 program) and area fraction of SPU covering the fractured surface area fraction was then calculated.

The fractured mode of the Ti-SPU composite and the chemical bonding state were characterized using XPS (SSI-SSX100). The take-off angle for photoelectron detection from the specimen surface was 35°. All binding energies given in this paper are relative to the Fermi level, and all spectra were excited with the monochromatized Al Kα line (1486.61 eV). The energy values were based on published data [1]. To estimate the photoelectron peak intensities, the background was subtracted from measured spectrum according to Shirley's method [2]. The composition and thickness of the surface oxide and the composition of the substrate were simultaneously calculated according to a method devised by one of the authors of this study [3-4]. Empirical data and theoretically calculated data of relative photoionization cross-sections were used for the quantification.

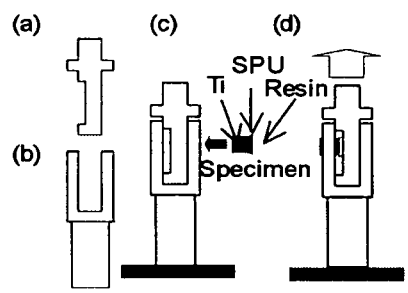

Fig. 1 Schematic image of the apparatus for adhesion shear test, (a) Moving and (b) fixed part . (c) The Ti-SPU composite was set through the holes on both parts which arraigned straight.(d) By pulling up of the moving part, shear stress was applied onto the boundary of composite.

Result and Discussion

Different thickness of γ-MPS layer with various immersion time and concentration of γ-MPS solution was shown in Fig.2. Even though the immersion time was increased, the thickness of γ-MPS layer was not significantly increased when immersed in 0.1, 0.5 or 1.0 % of γ-MPS solutions. However, the thickness of γ-MPS layer dramatically increased with longer immersion time when specimens were immersed in 2.0% γ-MPS solution. The thickness increased as the immersion time increase, but it decreased when immersion time was 100 min. It could be said that longer immersion time does not always increase the thickness of γ-MPS layer. The shear stress of the Ti-SPU composite increased with the increase of the concentration γ-MPS solution when the immersion time was limited for 1 min (data was not shown). The shear stress of Ti-SPU

composite immersed in 1.0, 2.0% γ-MPS solutions also increased with immersion times as shown in Fig.3. Furthermore, shear stress increased with the increase of thickness of γ-MPS layer as seen by the relation between shear stress of Ti-SPU composite and thickness of γ-MPS layer shown in Fig. 4.

Fig. 5 shows relation between shear stress and SPU area fraction to total fractured area of Ti-SPU composite. The shear stress was proportionally increased. Result could clarify that higher shear stress was observed on the Ti-SPU composite fractured at SPU area.

By XPS analysis, carbon, nitrogen, sulfur, silicon, and titanium were detected on the fractured surface. Table1 shows the ratios, [C-O, C-N, C=N]/[C], [C=O, OH^-, Si-O-Si]/[O], and [Ti^0]/[Ti] in the C 1s, O 1s and Ti 2p peaks, respectively, obtained from specimen with and without γ-MPS layer. [C-O, C-N, C=N]/[C], was significantly larger in Ti-SPU composite with the presence of γ-MPS layer. The C-O, C-N and C=N peaks were thought to originate from the SPU element. In other words, Ti-SPU composite was fractured remaining SPU element on the fractured surface regardless of γ-MPS layer. However, amount of residual SPU on the fractured surface of Ti-SPU composite with γ-MPS layer was more than that of Ti-SPU composite without γ-MPS layer. Regardless of γ-MPS layer, Ti^0 bond was detected on the fractured surface of Ti-SPU composites. The Ti^0 peak originated from the titanium metal substrate. Thus, the fracture layer that remained on the surface of Ti-SPU composite was very thin (less than 10 nm). Similar to [Ti^0]/[Ti], the proportional ratio of [C=O, OH^-, Si-O-Si]/[O] in the O 1s peaks was slightly larger in Ti-SPU composite with than without γ-MPS layer. The Si-O-Si peak originated from the γ-MPS layer. This is reason why proportional ratio of Ti-SPU composite with γ-MPS layer was bigger than that of Ti-SPU composite without γ-MPS layer.

The relative concentration of carbon, nitrogen, oxygen, sulfur, silicon and titanium in specimens were calculated and assumed that gross amount of these elements detected by XPS was 100 mol%. Table 2 presents the concentrations of carbon, oxygen and titanium on the fractured surfaces of Ti-SPU composite with or without γ-MPS layer. Carbon concentration originated from the SPU was significantly higher in Ti-SPU composite with the presence of γ-MPS layer. Moreover, large amount of SPU remained on the surface of Ti-SPU composite with γ-MPS layer compared to the Ti-SPU composite without γ-MPS layer. On the other hand, oxygen and titanium concentration decreased when γ-MPS layer was present. Using XPS, signals from titanium oxide and titanium substrate were small due to the remained layer.

Schematic model of Ti-SPU composite structure

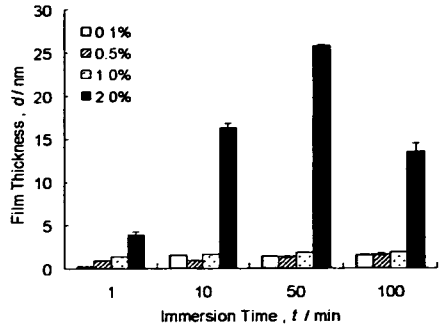

Fig.2 Thickness of the γ-MPS layer deposited on CP-Ti with various immersion time and concentration of γ-MPS solution.

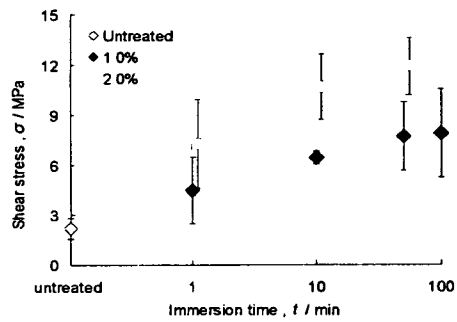

Fig.3 Shear stress of the Ti-SPU composite after immersion in 1.0, 2.0% γ-MPS solution at various immersion time.

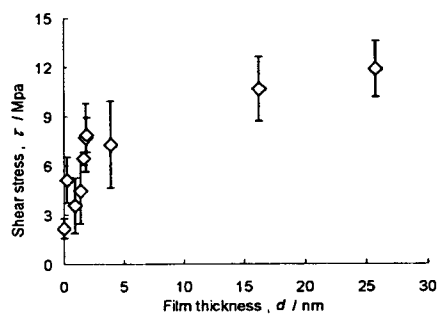

Fig. 4 Relation between shear stress and thickness of γ-MPS layer.

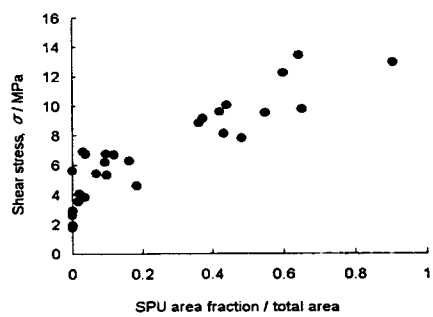

Fig. 5 Relation between shear stress and SPU area fraction to total fraction area.

through γ-MPS is shown Fig. 6. It is considered that a length of one molecular unit is more than 1 nm. If the numbers of one molecular unit per a unit surface area have not yet reached to maximum numbers, each molecular unit keeps distance from the their neighbors and is consequently allowed to lean on them. This could result, in the thin of γ-MPS layer (less than 1 nm). On the other hand, if the numbers of molecular unit will be become thicker layer(more than 1 nm). Thick γ-MPS layer has more molecular units bond to SPU. At thick γ-MPS layer, thus, shear stress of Ti-SPU composite was increased. SPU element remained on that fractured surfaces of Ti-SPU composite broken by shear force. This implies that b SPU area fraction remained on Ti-SPU composite, because of the γ-MPS layer. Furthermore, thicker γ-MPS layer coating, larger SPU area fraction was found.

Table 1 The proportional ratio of concentration of [C-O, C-N, C=N] / [C] ,[C=O, Si-O-Si, OH-] / [O] and [Ti^0] / [Ti] in fractured surface of the Ti-SPU composite. (number) mean ±S.D. * in the table represent significant differences between the corresponding. values (P<0.05)

	Area (%)		
	C	O	Ti
	C-O, N-C, N=C	C=O,OH,Si-O-Si	Ti^{0+}
without γ-MPS layer	20.6 (0.2) *	44.7 (5.6)	5.2 (0.1)
with γ-MPS layer	25.5 (0.9) *	50.7 (3.8)	6.2 (0.8)

Table 2 XPS results for relative concentration of elements in fractured surface of the Ti-SPU composite.(number) mean ± S.D. * in the table represent significant differences between the corresponding. values (P<0.05)

	Concentration (at%)		
	C	O	Ti
without γ-MPS layer	43.9 (2.0) *	42.4 (1.5) *	3.9 (0.1)
with γ-MPS layer	56.9 (1.3) *	35.7 (1.2) *	2.8 (1.0)

Summary

Thickness of γ-MPS layer could be controlled by immersion time and concentration of γ-MPS solution. Shear stress of Ti-SPU composite was increased with thickness of γ-MPS layer. It is considered that many molecular unites bonded with the SPU stands straight on the limited surface area, and resulted in to become thicker γ-MPS layer, while less molecular unites on the SPU easily leant to neighbor, and resulted in to become thinner γ-MPS layer apparently. This study revealed that γ-MPS is very useful to improve the adhesion strength of Ti-SPU composite for artificial implants. Factors governing shear bonding strength between Ti and SPU was thickness of γ-MPS layer.

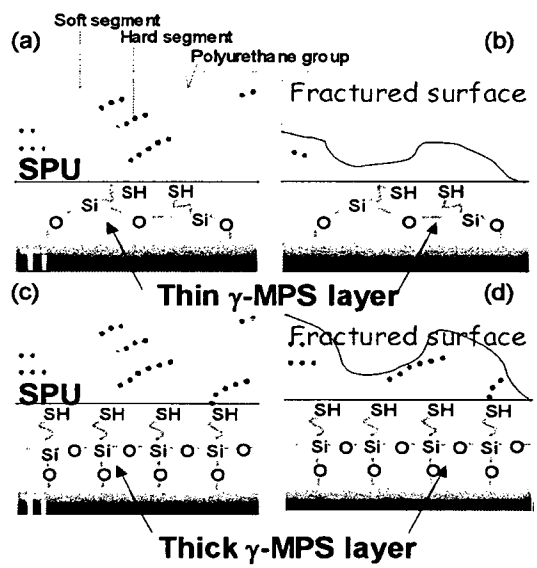

Fig. 6 Schematic model of the Ti-SPU composite structure through γ-MPS (a) Thin and (c) thick layer. Fractured surface of Ti-SPU composite after adhesion shear test.(c) thin and (d) thick layers of γ-MPS.

Rifference

[1] K. Asami, J: Electron Spectrosc. Vol. 9 (1976), p.469-478.
[2] D.A. Shirley: Phys. Rev. B5 (1972), p. 4709-4714
[3] K. Asami, K. Hashimoto and S. Shimodaira: Corr. Sci. Vol. 17 (1977), p. 713-723
[4] K. Asami and K. Hashimoto: Corros. Sci. Vol. 24 (1984), p. 83-97

Materials Science Forum Vols. 561-565 (2007) pp. 1477-1480
online at http://www.scientific.net

Online available since 2007/10/02

EFFECTS OF CROSS-LINKAGE AND HYDROXYL GROUPS ON BONDING STRENGTH BETWEEN TITANIUM AND SEGMENTED POLYURETHANE THROUGH 3-(TRIMETHOXYSILYL) PROPYL METHACRYLATE

Harumi Sakamoto[1, a], Yohei Hirohashi[2,b], Hisashi Doi[1,c], Kazuhiko Noda[2,d] and Takao Hanawa[1,e]

[1]Institute of Biomaterials and Bioengineering, Tokyo Medical and Dental University, JAPAN

[2]Department of Materials Science and Engineering, Shibaura Institute of Technology, JAPAN

[a]sak-met@tmd.ac.jp, [b]c03109@sic.shibaura-it.ac.jp, [c]doi.met@tmd.ac.jp,

[d]knoda@sic.shibaura-it.ac.jp and [e]hanawa.met@tmd.ac.jp

Keywords: Titanium, Segmented polyurethane, Silane coupling agent, Active hydroxyl groups, and Cross-links

Abstract. To create a new material with good biocompatibility and high mechanical strength for artificial organs, titanium (Ti) and segmented polyurethane (SPU) were bonded through 3-(trimethoxysilyl) propyl methacrylate (γ-MPS), and specify causes governing the bonding strength of Ti/γ-MPS/SPU interface. The number of cross-links of SPU and the concentration of active hydroxyl groups on the surface oxide film of Ti were controlled by UV-irradaiton and hydrogen peroxide immersion. The number of cross-links of SPU was measured by differential scanning calorimetry (DSC) and the concentration of the active hydroxyl groups was also determined using a zinc-complex substitution technique. Consequently, Ti/γ-MPS/SPU shear bonding stress was increased with the increase of the number of cross-links of SPU. In addition, the increase of cross-links in SPU also improved the Ti/γ-MPS/SPU shear bonding stress.

Introduction

Metals are widely used as biomaterials because of their high mechanical properties, especially toughness and long-term durability. However, the biocompatibility of metals is generally inferior to that of polymers and ceramics because no biofunction is added to metals during their manufacturing process. In order to expand the clinical application of metals, the biocompatibility of metals must be improved. On the other hand, polymers have been widely used since they have a high degree of flexibility and biocompatibility. If a metal and a polymer could be bonded and used as a composite material, a new material having good biocompatibility and high mechanical strength could be created. The encompassing clarification of the causes governing the bonding strength of the interface is one of the most challenging aspects to develop composite materials between metals and polymers.

The bonding of metals with polymers is currently utilized in dentistry. In particular, silane coupling agents are comprehensively used to combine metals with polymers. However, few reports have examined and discussed the chemical structures at the bonding interface and how they influence the bonding strength.

In a previous study[1], the unequivocal relationship between the shear bonding stress and the chemical structure at the bonding interface of a Ti- segmented polyurethane (SPU) composite using a silane coupling agent (γ-(trimethoxysilyl) propyl methacrylate: γ-MPS) was investigated. One of the causes governing the shear bonding stress between Ti and SPU is thickness of the γ-MPS layer.

The objective of this study was to investigate the effect of active hydroxyl groups on the surface oxide film of Ti and cross-links of SPU on the shear bonding stress of the interface in Ti-SPU

composite. The number of cross-links of SPU was measured by differential scanning calorimetry (DSC) and the concentration of the active hydroxyl groups on the surface oxide film was also determined with the zinc-complex substitution technique [2]. The shear bonding stress between Ti and SPU in Ti-SPU composites manufactured under various bonding conditions was evaluated.

Material and Methods

UV-irradiation treatment.

Commercially pure Ti disks with 2-mm thickness and 8-mm diameter (grade 2; Rare Metallic Co., Inc., Japan) were metallographically polished. 0.1, 1.0, and 2.0vol.% γ-MPS (Kanto Chemical Co., Inc., Japan) was prepared by diluting with deionized water and adjusted to pH 4.0 using acetic acid. Ti disks were immersed in 0.1 vol.% γ-MPS for 1 min (A), in1.0vol.% γ-MPS for 1 min (B), and in.2.0ovol.% γ-MPS for 50 min (C). According to previous research[1], it is predicted that the thickness of the γ-MPS layer on the Ti disks was the largest in this order:C, B, A.

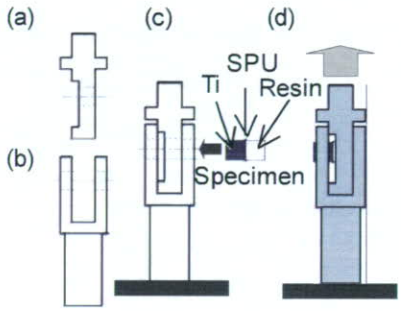

Fig. 1 Schematic image of the apparatus for adhesion shear test, (a) Moving and (b) fixed part. (c) The Ti-SPU composite was set through the holes on both parts which arraigned straight. (d) By pulling up of the moving part, shear stress was applied onto the boundary of composite.

To prepare a 3vol.% SPU solution, 600 mg Corethane70A (Crovita, USA), 10 mL tetrahydrofuran (Kanto Chemical Co., Inc., Japan), and 10 mL dimethylformamide (Kanto Chemical Co., Inc., Japan) were mixed. The Ti disks coated with γ-MPS were then immersed in the SPU solution for 2 d. Ti disks bonded to SPU were irradiated using a UV irradiation unit (Labolight, GC, Japan) for 20 s, 40 s .60 s, and 80 s. The grip for the shear bonding tests was formed on the outer surface of the SPU layer using an autopolymerized acrylic resin (UNIFAST II, GC, Japan). The shear bonding stress of the Ti/γ-MPS/SPU interface of the Ti-SPU composite was evaluated using a universal mechanical test machine (2000-IB, Shimadzu, Japan) with a crosshead speed of 0.1 mm min^{-1} at ambient temperature (Fig. 1).

SPU sheets were manufactured to determine the glass transition temperature (T_g) of SPU. 10 mL of the 3% SPU solution was dried in the vacuum desiccator for 2 d to obtain SPU sheets. UV was irradiated onto 10-mg SPU sheets for 0 s, 60 s, and 900 s. DSC (DSC7000, ULVAC, Tokyo) was carried out under a nitrogen atmosphere from −100 °C to 100 °C at a heating rate of 20 °C min^{-1}. T_g was determined as the intersection of the forward-extrapolated baseline with the backward-extrapolated initial slope of the peak.

Hydrogen peroxide immersion treatment.

The concentration of active hydroxyl groups could increase by immersion into a hydrogen peroxide (H_2O_2) solution [3]. Ti disks were immersed in a 3vol.% H_2O_2 solution (Kanto Chemical Co., Inc., Japan) at 303 K for 1 h, 24 h, 48 h, and 72 h to control the concentration of active hydroxyl groups on Ti. The chemical state of the surface oxide of the H_2O_2 treated Ti was determined using X-ray photoelectron spectroscopy (XPS, SSX100, SSI, UK) and the concentration of active hydroxyl groups existing on the surface oxide film on Ti disks was determined using a zinc complex substituting technique. The H_2O_2-treated Ti disks were immersed in a γ-MPS solution and bonded to SPU as described above. After the grips had been formed, the shear bonding test of the Ti/γ-MPS/SPU interface was carried out in the same manner as described above.

Result and Discussion

Effect of UV irradiation on Ti-SPU composite.

The relationships between the UV irradiation time and the shear bonding stress of the Ti/γ-MPS/SPU interface are shown in Fig. 2. Regardless of the thickness of the γ-MPS layer, the shear bonding stress of the Ti/γ-MPS/SPU interface increased with the UV-irradiation time. However, it decreased at 80s irradiation (A and B) and 60 s irradiation (C). The optimal UV-irradiation times were 60 s (A and B) and 40 s (C).

The typical thermal analysis curves around the T_g region are shown in Fig. 3. The T_g of SPU without UV irradiation, that with 1-min irradiation, and that with 15min irradiation were –54.3 °C, –49.1 °C, and –53.0 °C, respectively. The T_g of SPU increased with the UV irradiation. However, the T_g decreased after long irradiation.

It was considered that UV irradiation increased the number of cross-links in SPU, in other words, the degree of apparent polymerization. Therefore, the determination of the T_g of SPU was carried out using DSC. It is widely known that T_g increases with the increase in the number of cross-links in a polymer. Consequently, it was revealed that T_g and the number of cross-links in SPU increased at the optimal UV irradiation. However, T_g decreased with excessive irradiation of UV. This indicated that excessive UV irradiation decreased the number of cross-links, *i.e.*, the degree of apparent polymerization. Furthermore, the SPU deteriorated with UV irradiation.

Schematic illustrations of the effects of UV irradiation on the Ti/γ-MPS/SPU interface are shown in Fig. 4. Hydrophobic CH_2 groups of SPU and γ-MPS existed as mutually intertwined. These intertwining CH_2 groups consolidated more when the number of cross-links in SPU increased with UV irradiation (Fig. 4(b)). Therefore, the shear bonding stress of the TI/γ-MPS/SPU interface increased with UV irradiation.

Effect of hjydroxly groups on Ti-SPU composite.

The O 1s electron energy region peak contained three component peaks originating from oxide, O^{2-}, hydroxide or hydroxyl groups, OH^-, and hydrate and/or adsorbed water, H_2O. The ratios of $[O^{2-}]/[O]$, $[OH^-]/[O]$, and $[H_2O]/[O]$ on the surface oxide film of Ti disks plotted against the H_2O_2-treatment time are shown in Fig. 5. In a Ti disk with H_2O_2 treatment for 1 h, the $[O^{2-}]/[O]$ increased, whereas the $[OH^-]/[O]$ and the $[H_2O]/[O]$ decreased. With the H_2O_2 solution as an oxidant, the oxidation of the surface oxide film progressed. Each ratio was almost constant up to 48 h. The surface oxide film of Ti disks was completely oxidized and consisted of only TiO_2. The $[O^{2-}]/[O]$ and $[OH^-]/O]$

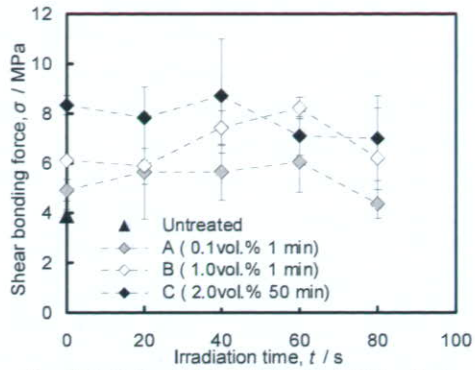

Fig. 2 Relationship between the UV-irradiating time and the shear bonding stress of the Ti/γ-MPS/SPU interface of the Ti-SPU composite. immersed in (A) 0.1%/γ MPS for 1 min, (B) 1.0% γ-MPS for 1 min, and (C) 2.0%γ-MPS for 50 min.

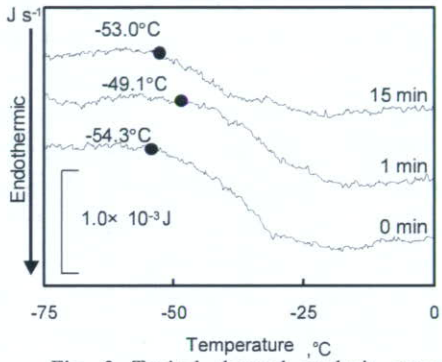

Fig. 3 Typical thermal analysis curve around the T_g region.

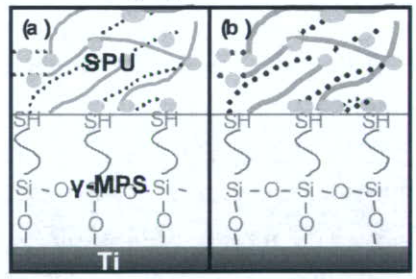

Fig. 4 Schematic model of Ti/γ-MPS/SPU interface structure through γ-MPS. (a) Untreated , (b) UV-irradiation.

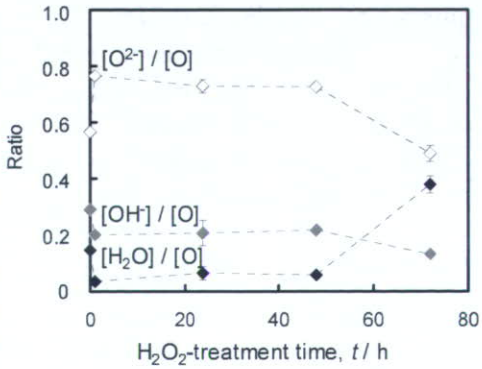

Fig. 5 Ratio of the proportion of the concentration of O^{2-} to that of O, OH^- to that of O, and H_2O to that of O in surface oxide film on Ti disks plotted against H_2O_2 treatment time.